第 34 卷第 4 期
2015 年 8 月

红 外 与 毫 米 波 学 报
J. Infrared Millim. Waves

Vol. 34, No. 4
August, 2015

文章编号: 1001 - 9014(2015)04 - 0401 - 05　　DOI:10.11972/j.issn.1001 - 9014.2015.04.004

Adaptive nonuniformity correction algorithm based on multiscale temporal moment matching

LENG Han-Bing*, HU Bing-Liang, ZHOU Zuo-Feng, TANG Li-Nao, ZHANG Jian, YAN A-Qi

(Xi'an Institute of Optics and Precision Mechanics, Chinese Academy of Sciences, Xi'an, 710119, China)

Abstract: The fixed pattern noise of uncooled infrared focal plane arrays has the similar characteristics with the stripe noise. By researching the moment matching and temporal high-pass filter, a novel multiscale temporal moment matching nonuniformity correction algorithm was proposed. In the proposed algorithm, global motion was first identified by the Gaussian pyramid of the adjacent uncorrected images. Then the temporal moment matching was performed in all levels of Gaussian pyramids and Laplacian pyramids. The experimental results with the real infrared video sequences have shown that the proposed algorithm can significantly increase the convergence speed and reduce the ghosting artifacts.

Key words: nonuniformity correction, temporal high-pass filter, multiscale temporal moment matching, Laplacian pyramid, ghosting artifacts

PACS: 07.07. Kp

基于多尺度时域矩匹配的自适应非均匀性校正算法

冷寒冰*，胡炳樑，周祚峰，唐利孬，张　建，闫阿奇

(中国科学院西安光学精密机械研究所,陕西 西安　710119)

摘要:非制冷红外焦平面阵列的固定图案噪声具有与条带噪声相类似的特性.通过对矩匹配算法和时域高通滤波算法的研究,提出了一种多尺度时域矩匹配非均匀性校正算法.首先利用高斯金字塔对相邻帧待校正图像进行全局运动估计,然后对各尺度的高斯金字塔和拉普拉斯金字塔分别进行时域矩匹配.对真实红外图像序列的实验结果表明,该算法在提高收敛速度的同时可有效减少鬼影现象的出现.

关　键　词:非均匀性校正;时域高通滤波;多尺度时域矩匹配;拉普拉斯金字塔;鬼影

中图分类号:TN911.73　　**文献标识码**:A

Introduction

The uncooled infrared focal plane arrays (IRFPAs) are widely used in a variety of applications such as remote sensing, surveillance and so on. Due to the fixed pattern noise (FPN) is always decreasing the temperature resolution of infrared imaging systems, nonuniformity correction (NUC) technique is an essential way to increase the image quality. Currently, the NUC algorithms can be divided into two categories: reference-based NUC and scene-based NUC. Reference-based NUC mainly consist one point correction (OPC) and two point correction (TPC). Scene-based correction mainly consist statistical methods and registration-based methods. Statistical methods, such as temporal high-pass filtering NUC (THPF-NUC)[1], constant statistics method[2], generally require the relative motion between target scene and IRFPA camera. Registration-based correction algorithm, such as algebraic method, inter-frame registration method[3], usually require complex computation, and the correction errors are transmitted accumulatively step by step, which makes these methods difficult to achieve a practical effect.

In this paper, we proposed a novel multiscale temporal moment matching NUC (MTMM-NUC) algorithm for uncooled IRFPAs. The remainder of this paper is organized as follows. In Sec. 1, the moment matching NUC (MM-NUC) algorithm and its shortcomings are analyzed. In Sec. 2, a novel MTMM-NUC algorithm is de-

Received date: 2014 - 05 - 25, **revised date**: 2015 - 06 - 06　　**收稿日期**:2014 - 05 - 25, **修回日期**:2015 - 06 - 06

Foundation items: National Natural Science Foundation of China (61201376) and Western Light project of CAS (Y229E21213)

Biography: LENG Han-Bing(1978-), male, associate researcher, Ph. D, mainly focused on infrared system design

* **Corresponding author**: E-mail: lenghanbing@opt.ac.cn

scribed in detail. The experiments with real IR image are given in Sec. 3, and finally there comes the conclusion in Sec. 4.

1 Moment matching NUC algorithm

Linear model is often used in IRFPA NUC algorithm. For each (i,j)th detectors in the IRFPA, assume that the original uncorrected gray value is $X(i,j)$, the linear NUC formula is given in Eq. 1.

$$Y(i,j) = g(i,j)X(i,j) + b(i,j) \quad , \quad (1)$$

where the variable $g(i,j)$ represents the gain of the (i,j)th detectors and $b(i,j)$ is the offset of the detectors, $Y(i,j)$ stands for the corrected image, M and N are row and column number, $i = 1,2,\cdots,M; j = 1,2,\cdots,N$.

Considering the fact that in uncooled IRFPA's read out circuit, the pixels in the same column always share the same amplifier, therefore the gain and the offset of the same column are almost equal. Then the NUC formula can be converted to Fq. 2,

$$Y(i,j) = g(j)X(i,j) + b(j) \quad , \quad (2)$$

where the j-th column detectors share the same gain $g(j)$ and the same offset $b(j)$.

The MM-NUC method is based on the assumptions that the images have to be sufficiently large, the distribution of all objects is homogeneous, and each detector responds linearly to the level of incoming radiation. Ignoring the influence caused by noises, the pixel gray value can be expressed as a linearity of the sensor gain and offset. The mean and standard deviation value of the whole image are often treated as the reference, then the means of columns and standard deviations are stretched to the same reference, thus the stripe noise is removed.

$$g(j) = \sigma(r)/\sigma(j) \quad , \quad (3)$$

$$b(j) = \mu(r) - \mu(j)\sigma(r)/\sigma(j) \quad . \quad (4)$$

Equations 3 ~ 4 shows the correction coefficients obtained from MM-NUC method. $\sigma(r)$ and $\mu(r)$ are the standard deviation and mean value of the image $X(i,j)$, $\sigma(j)$ and $\mu(j)$ are the standard deviation and mean value of the j-th column. As a matter of fact, MM-NUC is only effective under the conditions that the image is quite large and the objects have uniform distribution, which are almost impossible to be satisfied in real applications.

Currently, the MM-NUC method is mainly applied on huge resolution remote sensing images, and some effective improvements have been proposed by researchers. Qin[4] proposed an improved piece-wise linear dynamic moment matching (PWMM-NUC) algorithm. The image is directly segmented into three regions: low region, median region and high region, then MM-NUC method is applied to three regions separately. The accuracy of image segmentation is severely affected by the stripe noise, and this often leads to the consequence of that the stripe noise can not be removed completely. The other improved algorithms are also based on single image processing, and they can hardly resolve the "edge effect" problem thoroughly.

2 THPF-NUC and its improvements

As the inspiration of the proposed MTMM-NUC algorithm comes from the THPF-NUC algorithm, we first reviewed the THPF-NUC algorithm and its improvements. THPF-NUC is a classical scene-based adaptive NUC algorithm, its realization[1] can be achieved by Eqs. 5 ~ 6, where $f(i,j)$ is a recursive IIR filter.

$$Y_n(i,j) = X_n(i,j) - f_n(i,j) \quad , \quad (5)$$

$$f_n(i,j) = \frac{1}{K}X_n(i,j) + (1-\frac{1}{K})f_{n-1}(i,j) \quad , \quad (6)$$

here $X_n(i,j)$ is the input image and $Y_n(i,j)$ is the corrected output, K is frame index, is the time constant. In the THPF-NUC algorithm, the key component is the recursive equation, Eq. 6 shows. The uncorrected image $X_n(i,j)$ is directly participated in the recursive procedure. If there are insufficient motions or excessively strong scene values in the frames, the algorithm will essentially fade out the stationary image and affect the convergence process.

Qian[1] proposed an improvement of the THPF-NUC algorithm by replacing the $X_n(i,j)$ with its high spatial frequency, it was called space low-pass and temporal high-pass algorithm (SLTHP-NUC). The key recursive equation is listed in Eq. 7, where $X_n^{\mathrm{HSF}}(i,j)$ is the high spatial frequency of the $X_n(i,j)$. Zuo[5] also proposed an new THPF-NUC algorithm based on bilateral filter (BFTH-NUC), the key recursive equation is shown in Eq. 8, where X_n^{BFr} represent the residual of the bilateral filter.

$$f_n(i,j) = \frac{1}{K}X_n^{\mathrm{HSF}}(i,j) + (1-\frac{1}{K})f_{n-1}(i,j) \quad , (7)$$

$$f_n(i,j) = \frac{1}{K}X_n^{\mathrm{BFr}}(i,j) + (1-\frac{1}{K})f_{n-1}(i,j) \quad . (8)$$

The characteristic of the improvements mentioned above is that in the recursive process, the original uncorrected image is replaced by the output of a filter. These improvements could significantly increase the convergence speed and reduce the emergence of the "ghosting artifacts" compared with the original THPF-NUC algorithm. However when the IR camera is stationary or moves fast, the corrected image still has "image bending" and "ghosting artifacts."

3 MTMM-NUC algorithm

The MTMM-NUC algorithm is similar to the THPF-NUC method, the difference between them is that the gray value directly participates in the recursive process in THPF-NUC, while only some statistical characteristics participate in the recursive process in MTMM-NUC. The complete implementation process of MTMM-NUC consist four steps: (1) pyramid decomposition of the uncorrected image; (2) image motion detection; (3) correction coefficients updating; (4) image nonuniformity correction. The detailed description of the proposed algorithm is listed below.

3.1 Image pyramid decomposition

The pyramid structure was proposed by Burt and Adelson[6] to describe image, which possessed of multi-resolution characteristic. The basic principle of this method is to decompose the source image into pieces of sub-images with different spatial resolutions through some mathematical operations. To the original uncorrected image $X(i,j)$, through Laplacian pyramid decomposition, it could be represented as the following equation[7]:

$$X(i,j) = LP_1(i,j) + LP_2(i,j) + LP_3(i,j) + \cdots + LP_L(i,j) + \hat{X}_L(i,j) \quad , \quad (9)$$

where $LP_1(i,j)$ means the L level Laplacian pyramid and $\hat{X}_L(i,j)$ means the L level Gaussian pyramid.

Figure 1(a) shows an uncorrected infrared image obtained from an uncooled microbolometer. The pyramid decomposition level is 3, Fig. 1(b) ~ Fig. 1(d) shows the Laplacian pyramid LP_1, LP_2 and LP_3 separately (the (i,j) is omitted here for simplicity), Fig. 1(e) shows the Gaussian pyramid $\hat{X}_3$. From the images we can see, the stripe noise has stronger visual impact on Lapacian pyramid than on Gaussian pyramid. Removing stripe noise in all pyramid images and then reconstructing, the denoised image could be obtained.

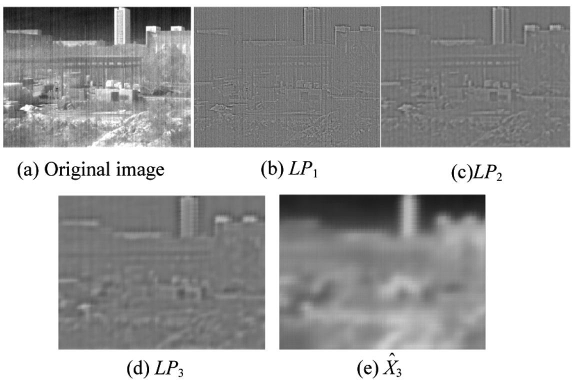

Fig. 1 Pyramid decomposition result
图 1 金字塔分解结果 (a)原图, (b) LP_1, (c) LP_2, (d) LP_3, (e) $\hat{X}_3$

3.2 Image motion detection

The image motion is much complicated in variety of real applications. The ghosting artifacts always occurs when the IR camera is recording objects that are not moving with respect to the camera and then they suddenly leave the field of view. Harris[8] has proposed a motion detection method based on the difference of the adjacent image frames, the changes of each pixel was compared with a threshold value, and the correction coefficients will only update if the change is greater than the threshold. This method prevents biased estimates from stationary objects in scenes and helps to sample data better. The disadvantage of this method is that the differences of the adjacent frames are deeply affected by the random noise, the proper threshold is hard to be obtained. This paper proposed a new motion detection method, the main idea is to pick out the global moving information other than the changing pixels.

Assume the adjacent Gaussian pyramids mentioned in the former section are $\hat{X}_3(n\text{-}1)$ and $\hat{X}_3(n)$, represents the frame number. Sobel edge detection operator is then separately performed to the two adjacent frames, here we use $E_{n\text{-}1}(i,j)$ and $E_n(i,j)$ to represent the edge detection result. If the total number of coincidence edge pixels *pBoth* in the two frames satisfies the Eq. 10, the current frame is determined to be "motionless", and set moving flag $F=0$, else it is determined to be "moving", and set moving flag $F=1$. In Eq. 10, $pE(n)$ represents the total number of edge pixels in $E_n(i,j)$, δ is an empirical value, usually set to 0.96.

$$\frac{p\mathrm{Both}}{(pE(n\text{-}1)/2 + pE(n)/2)} \geqslant \delta \quad . \quad (10)$$

The proposed global motion detection method is insensitive to the random noise, and the threshold is affected little by the random noise compared with the Harris's method.

3.3 Correction coefficients updating

Similar to the recursive Eq. 6 ~ 8, the correction coefficients updating equation in the proposed MTMM-NUC are presented in Eq. 11 ~ 12.

$$\begin{cases} \mu_n(j) = \frac{1}{K}\mu_n(j) + (1\text{-}\frac{1}{K})(\mu_{n\text{-}1}(j)\text{-}\mu_n(j)) \\ \sigma_n(j) = \frac{1}{K}\sigma_n(j) + (1\text{-}\frac{1}{K})(\sigma_{n\text{-}1}(j)\text{-}\sigma_n(j)) \end{cases} \text{when } F=1 \quad , \quad (11)$$

$$\begin{cases} \mu_n(j) = \mu_{n\text{-}1}(j) \\ \sigma_n(j) = \sigma_{n\text{-}1}(j) \end{cases} \text{when} \quad F = 0 \quad , \quad (12)$$

where the $\mu_n(j)$ represents the j-th column average gray value of the n-th frame $X_n(i,j)$, $\sigma_n(j)$ represents the j-th column standard deviation of the n-th frame. When the IR camera is moving, the Eq. 11 is used to update the correction coefficients. When the camera is motionless, the Eq. 12 is used. The corrected output $Y_n(i,j)$ is given in Eq. 13.

$$Y_n(i,j) = \frac{\sigma_n(r)}{\sigma_n(j)}X_n(i,j) + \mu_n(r) - \frac{\sigma_n(r)}{\sigma_n(j)}\mu_n(j) \quad . \quad (13)$$

As the original image $X_n(i,j)$ is decomposed to LP_1, LP_2, LP_3, $\cdots$, LP_L and $\hat{X}_L$, the Eq. 13 is then applied to the $L+1$ pyramids separately. Assume the corrected output are LP'_1, LP'_2, $\cdots$, LP_L and $\hat{X}'_L$, the final output Y'_n of the proposed MTMM-NUC is

$$Y'_n = LP'_1 + LP'_2 + LP'_3 + \cdots + LP'_L + \hat{X}'_L \quad . (14)$$

4 Experiments and results

We used the IR camera mentioned in the Sec. 1 to obtain a series of uncorrected video sequences. The bad pixels of the IRFPA were picked out and compensated with the adjacent normal pixels, and then the NUC algorithm mentioned above was separately performed. In SLTHP-NUC, BFTHP-NUC and the proposed MTMM-NUC, the time constant is 33. A threshold of $Th = 150$ is used in SLTHP-NUC, while the BFTHP-NUC uses $D = 15$, $\sigma = 2.5$, $\sigma_r = 150$.

The video sequence is about 1125 frames. The IR camera keeps moving from frame 1 to frame 946, while keeps motionless from frame 947 to frame 1125. In order to evaluate the convergence speed, we assume that there is no response drifting in such a short period, and the TPC result of the original sequence is used as a reference. The root-mean-square error (RMSE) is adopted for measurement of the NUC performance. RMSE is defined as follows:

$$\mathrm{RMSE} = \sqrt{\frac{1}{M \times N}\sum_{i,j}(I(i,j)\text{-}I_{\mathrm{TPC}}(i,j))^2} \quad ,(15)$$

where $I_{(}i,j)$ is the (i,j) pixel value of the original image while $I_{TPC}(i,j)$ is the corrected result of the TPC algorithm.

Figure 2 shows the NUC result of the frame 900, and Fig. 3 shows the NUC result of the frame 1100. The correction result of the MM-NUC is poor no matter the scene is moving or motionless, "Edge effect" is very obvious. The PWMM-NUC can only remove most of the stripe noise, and there still have some stripe noise left both in moving and motionless scene. SLTHP-NUC is recommended to combined with OPC method in real application in Qian's[1] paper. Figure 2 (d) shows the result when it is used without OPC method. From the image we can see, most of the stripe noises can be removed but there still left a few stripe noises. Its drawbacks are that when the camera comes into the motionless state, the images gradually fade out and blurred. Although Qian introduced a motion detection technique in SLTHP-NUC, each pixel in two neighboring frames is compared with a fixed threshold. Even though the correction coefficients only are updated when the change is greater than the threshold, the ghosting artifacts still occurs especially when IR camera stops moving. The BFTHP-NUC has a better vision effect than the SLTHP-NUC when used in moving sequence. In motionless sequence, However, the stationary scenes also fade out and blurred, as Fig. 3 (e) shows. The proposed MTMM-NUC method manifest a better correction result both in moving and motionless scene, and almost no ghosting artifacts could be found in Fig. 2 (f) and Fig. 3 (f).

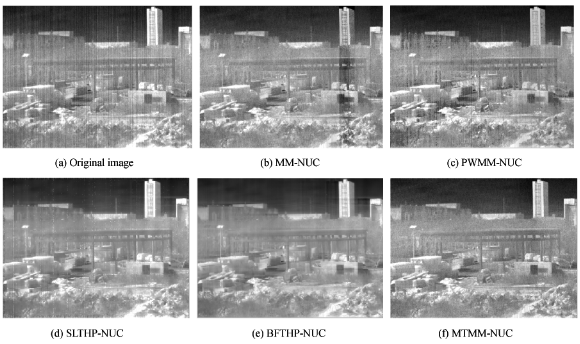

Fig. 2 NUC results in moving sequence (frame 900th)
图 2 运动序列非均匀性校正结果(第 900 帧)

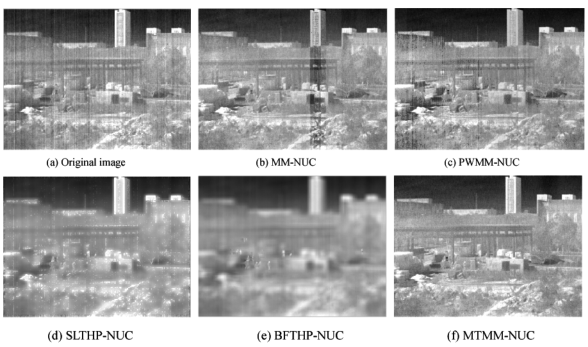

Fig. 3 NUC results in static sequence (frame 1100th)
图 3 静止序列非均匀性校正结果(第 1100 帧)

The RMSE versus frame numbers of the mentioned algorithms are shown in Fig. 4. The MM-NUC and PWMM-NUC is single frame processing method, and they do not have the problem of convergence speed and ghosting artifacts. However their correction effects are poorer compared with the other methods. The SLTHP-NUC and BFTHP-NUC only need about 50 frames to reach convergence, and this has already been proved in Qian's[1] and Zuo's[5] paper. The shortcomings of their algorithm are that when the scenes get into the motionless state, the RMSE increase due to the occurrence of the "image bending". Meanwhile, the proposed MTMM-NUC algorithm has no convergence problem, the correction coefficients could be obtained by the first frame, and then the second frame can achieve convergence immediately. Through the global motion detection method, little ghosting artifacts could be found in the corrected sequence.

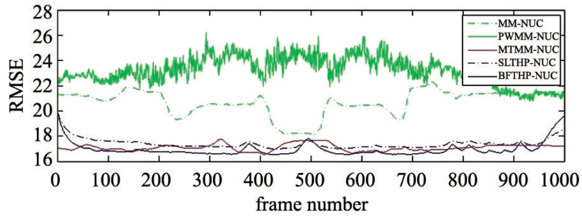

Fig. 4 RMSE versus the frame numbers for the five algorithms
图 4 5 种校正算法 RMSE 对比图

In the proposed MTMM-NUC algorithm, different pyramid decomposition level may result in the different correction effect. Through experiments, we found that 3 is the optimal decomposition level, compared with the calculation amount and the correction effect.

Table 1 gives the RMSE contrast of frame 900 and frame 1100. When the image sequences have global motion, the RMSE values of the SLTHP-NUC、BFTHP-NUC and MTMM-NUC only have small differences. When there is no global motion in the image sequences, the MTMM-NUC can give the smallest RMSE value. Considering the visual effect of the corrected images and the RMSE values listed in Table 1, a conclusion could be made that the MTMM-NUC is a more effective NUC method than the other algorithms mentioned above.

Table 1 RMSE of the NUC result for frame 900 and 1100
表 1 第 900 和第 1100 帧校正后的 RMSE

	MM-NUC	PWMM-NUC	SLTHP-NUC	BFTHP-NUC	MTMM-NUC
frame 900	21.2370	21.7288	17.3344	16.8288	17.0610

5 Conclusions

In this paper, a novel NUC algorithm called multi-scale temporal moment matching was proposed. By the pyramid decomposition, global motion detection was first performed, then the temporal moment matching was implemented in multiscale. The proposed algorithm has merits of fast convergence speed and almost no ghosting artifacts, no matter the scene is moving or motionless. Experiments on real IR sequences demonstrate the effectiveness of this method. This algorithm is simple for hardware implementation, and can improve the real-time performance of practical IR imaging systems. The future work will be focused on the effectiveness verification of the different kind of complex scenes.

References

[1] Qian W X, Chen Q, Gu G. Space low-pass and temporal high-pass nonuniformity correction algorithm [J]. *Optical Review*, **17**(1), 2010:24-29.

[2] Qian W X, Chen Q, Gu G H. The high-frequency constant-statistics constraint nonuniformity correction algorithm [J]. *J Infrared Milli Terahz Waves*, 2011, **32**: 778-792.

[3] Zuo C, Chen Q, Gu G H, *et al*, scene-based nonuniformity correction algorithm based on interframe registration [J]. *J. Opt. Soc. Am.* A, **28**(6), 2011: 1164-1176.

[4] Qin Y, Deng R R, He Y Q, *et. al*, Piece-wise linear dynamic moment matching destriping [J]. *Journal of Image and Graphics*, **17**(11), 2012: 1444-1452.

[5] Zuo C, Chen Q, Gu G H, *et. al*, New temporal High-pass filter nonuniformity correction based on bilateral filter [J]. *Optical Reviews*, **18**(2), 2011: 197-202.

[6] Kumari S, Malviya M, Lade S. Image Fusion techniques based on pyramid decomposition [J]. *International Journal of Artificial Intelligence and Mechatronics*, 2014, **2**(4): 127-130.

[7] Wang W C. A Multi-focus Image Fusion Method Based on Laplacian Pyramid [J]. *Journal of computers*, 2011, **6**(12): 2559-2566.

[8] Harris J G, Chiang Y M, Minimizing the "ghosting" artifact in scene-based nonuniformity correction [C]. *Proc. SPIE*, 1998, 3377: 106-113.